Paper 10

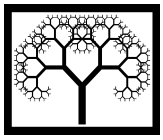

Proceedings of the Eleventh International Conference
on Computational Structures Technology,
B.H.V. Topping, (Editor),
Civil-Comp Press, Stirlingshire, Scotland

Shear Strength of End Web Panels

S.S. Safar
Construction and Architectural Engineering Department
American University in Cairo, Egypt

Abstract

In most classical failure theories for post-buckled web panels subjected to pure shear, it was assumed that diagonal tension strip was anchored by flanges and, or adjacent web panels. Such an assumption led to the conclusion that post-buckling strength can only develop in intermediate web panels. Accordingly, the AISC specification do not account for post-buckling strength in proportioning end web panels. In this paper, the shear strength of perfect end web panels stiffened with end-bearing and transverse stiffeners was investigated using the finite element method. The analysis accounts for both geometric and material non-linearities. Numerical results were verified by comparison with classical theory and experimental results published in the literature. Contrary to most post-buckling theories, it was shown that end web panels developed tension field action after buckling and principal tensile stresses were balanced by growing compressive stresses in end-bearing stiffeners and portions of the web stiffened by flanges and stiffeners. An extensive parametric analysis was conducted on end web panels to assess the effect of geometric parameters on shear strength. Numerical results were used to establish a mathematical expression for the ultimate shear strength of perfect end-web panels including tension field action.

Keywords: post-buckling, shear strength, non-linear analysis, finite element analysis, tension field action, end-bearing stiffener.

1 Introduction

Experimental and numerical research work on transversally stiffened plate girders revealed that they can support shear loads after web buckling [1-6]. Hence the ultimate shear strength of web panels, V_n, was computed by adding the elastic buckling load, V_{cr} and the post-buckling strength, V_{pb} [7]. Timoshenko and Gere [8] established a closed form solution for V_{cr} using classical elastic theory as follows:

$$V_{cr} = ht_w K \frac{\pi^2 E}{12\left(1-\mu^2\right)\left(h/t_w\right)^2} \tag{1}$$

where E is the modulus of elasticity, μ is Poisson's ratio, h is the depth of the plate girder web, and t_w is thickness of the web. The buckling coefficient, K, depends on the boundary conditions of the web panel and its aspect ratio, a/h, where a is the spacing between transverse stiffeners. The buckling coefficients based on simply supported boundary conditions, K_{ss}, and fixed boundary conditions, K_{sf}, at flanges were derived [8, 9] for $a/h \geq 1$ as follows:

$$K_{ss} = 5.34 + \frac{4}{\left(a/h\right)^2} \tag{2}$$

$$K_{sf} = \frac{5.61}{\left(a/h\right)^2} - \frac{1.99}{\left(a/h\right)^3} + 8.98 \tag{3}$$

Numerical research work on transversally stiffened web panels revealed that when practical plate girder flange dimensions were used, the web boundary conditions at flanges were closer to fixation [1, 5, and 6]. Therefore, Lee and Yoo [1] assumed 80% fixation of the web at flanges and determined K in Equation (1) as follows:

$$K = K_{ss} + 0.8\left(K_{sf} - K_{ss}\right) \tag{4}$$

The American Institute for Steel Construction [10], AISC, however, adopts an expression of K based on assuming simply supported boundary condition at flanges as follows:

$$\begin{aligned} K &= 5 + 5/(a/h)^2 \\ &= 5 \qquad \text{for } a/h > 3 \text{ or } a/h > (260/(h/t_w))^2 \end{aligned} \tag{5}$$

Based on such assumption, the AISC design rules underestimated V_{cr} obtained by numerical research work by 30% [5, 6].

Post buckling strength of web panels, V_{pb}, was first explained by Wagner in 1931 by assuming a uniform diagonal tension field developed in the web after buckling [7]. In 1961, it was noted by Basler that the diagonal tension field was limited to a portion in the web, he derived an expression for V_{pb} by assuming the diagonal tension field to be fully yielded and the vertical component of diagonal tension was equilibrated by axial compressive force supported by transverse stiffeners. In 1975, Porter et al. explained large flange deformations of web panels observed at ultimate load by sway mechanism where plastic hinges occurred in flanges that anchored diagonal tension after web buckling [7]. Both post-buckling theories were used as the basis for the provisions of shear strength of webs in current codes. Basler's theory was adopted in the AISC specifications whereas the Rockey, or Cardiff model (Porter et al.) was adopted in the British Standard, BS 5400. According to Basler's post-buckling theory, diagonal tension field can not develop

in the web without recourse of anchoring mechanism in flanges and adjacent web panels [11-13]. Therefore, ultimate shear strength of end web panels, V_n, was expressed without the tension field action terms in the AISC design equations as follows [10]:

$$V_n = 0.60 F_y h t_w C \tag{6}$$

where the coefficient, C, is the ratio of the buckling load to the yield load capacity of the web, $V_y = 0.6\ F_y\ h\ t_w$, and is determined according to governing failure mechanism based on the web plate slenderness ratio, h/t_w, as follows [10]:

I –*Yielding*
$$\frac{h}{t_w} \le 1.10\sqrt{\frac{Ek}{F_y}} \qquad C = 1.0 \tag{7a}$$

II – *Inelastic Buckling*
$$1.10\sqrt{\frac{Ek}{F_y}} < \frac{h}{t_w} \le 1.37\sqrt{\frac{Ek}{F_y}} \qquad C = \frac{1.10}{(h/t_w)}\sqrt{\frac{Ek}{F_y}} \tag{7b}$$

III – *Elastic Buckling*
$$\frac{h}{t_w} > 1.37\sqrt{\frac{Ek}{F_y}} \qquad C = \frac{1.51}{(h/t_w)^2}\left(\frac{Ek}{F_y}\right) \tag{7c}$$

The buckling coefficient in Equations (7) is computed from Equation (5) assuming simply supported boundary conditions. Recent experimental and numerical research work revealed many discrepancies between post-buckling theories and behaviour of transversally stiffened web panels. It was shown by Lee and Yoo [1] and others [5, 6, 14 and 15] that out-of-plane deformations in the web that occurred after buckling developed through thickness stresses that prohibited the diagonal tension strip from achieving full yield capacity. Therefore, it was proposed by Lee and Yoo [1] that the post-buckling strength of intermediate web panels should not exceed 0.4 ($V_y - V_{cr}$) and hence derived an expression for the ultimate shear strength of perfect intermediate web panels as follows:

$$V_n = 0.58 F_y h t_w \left[0.6C + 0.4\right] \tag{8}$$

where C was determined according to the governing failure mode as follows:

I –*Yielding*
$$\frac{h}{t_w} \le 1.11\sqrt{\frac{Ek}{F_y}} \qquad C = 1.0 \tag{9a}$$

II – *Inelastic Buckling*
$$1.11\sqrt{\frac{Ek}{F_y}} < \frac{h}{t_w} \le 1.39\sqrt{\frac{Ek}{F_y}} \qquad C = \frac{1.11}{(h/t_w)}\sqrt{\frac{Ek}{F_y}} \tag{9b}$$

III – *Elastic Buckling*
$$\frac{h}{t_w} > 1.39\sqrt{\frac{Ek}{F_y}} \qquad C = \frac{1.55}{(h/t_w)^2}\left(\frac{Ek}{F_y}\right) \tag{9c}$$

Based on numerical research work [11 - 15], it was reported that the anchoring mechanism of diagonal tension strip in flanges and adjacent panels was irrelevant to

post-buckling strength. Unlike most post-buckling theories, it was shown that web panels supported compressive stresses after buckling that balanced with diagonal tension stresses. It was reported by several investigators that the expected large compressive forces in transverse stiffeners did not exist but rather transverse stiffeners were essentially loaded in bending to prevent the web out-of-plane deformations after buckling [4, 15]. Therefore, the minimum area requirement stipulated on intermediate stiffeners to support vertical component of diagonal tension forces was irrelevant. The AISC [10] also stipulates minimum inertia, I_o, and width-to-thickness ratio, b_t/t_s, for transverse stiffeners to prevent flexural and local buckling due to axial compression as follows:

$$I_o \geq a\, t_w^{\,3} j \tag{10}$$

$$\frac{b_s}{t_s} \leq 0.56\sqrt{\frac{E}{F_{ys}}} \tag{11}$$

where $j = 2.5 / (a/h)^2 - 2 \geq 0.5$. Based on numerical and experimental work [4, 15], it was shown that I_o, of Equation (10) was not sufficient to develop the potential post-buckling strength of the web. Therefore it was proposed by several researchers [4, 15] to increase the inertia of intermediate stiffeners several times depending on h/t_w and a/h.

End-bearing stiffeners of plate girders were designed as per the AISC specifications to satisfy minimum area to transfer support reactions by bearing according to the following:

$$V_n \leq 2\, F_y\, A_{se} \tag{12}$$

where A_{se} is the total area of end-bearing stiffener. For single pair end-bearing stiffeners composed of two plates welded to the web, $A_{se} = 2b_{st}t_{st}$ where b_{st} and t_{st} is the width and thickness of each stiffener plate. The value of b_{se}/t_{se} should also satisfy Equation (11) to prevent local buckling. The cross section of end-bearing stiffeners should also be selected to prevent flexural buckling assuming an effective buckling length of $0.75h$ to account for partial fixation provided by the flanges. A strip with width $12t_w$ from the web was assumed to be a part of the stiffener cross sectional area in computing the slenderness ratio of exterior end-bearing stiffeners. The critical stress, F_{cr}, for end-bearing stiffeners was assumed similar to that adopted for compression members [10] except that it was set to F_y for slenderness ratio less than 25.

Alinia [14] demonstrated by finite element work that long web panels may possess post-buckling strength unlike the arbitrary limit imposed by Basler on the maximum aspect ratio of 3.0 that was adopted by the AISC.

In this work, the analysis of plate girders with transversally stiffened plate girders was conducted using the finite element method. The suitable element size that provides converged numerical solution was determined by conducting mesh sensitivity study. The finite element analysis results were verified by comparing the elastic buckling load to classical theory whereas ultimate load was compared to test results published in literature. The verified finite element model was used to conduct

an extensive parametric analysis to assess the effect of geometric parameters on shear strength of end-web panels. Numerical results were used to establish a mathematical expression for ultimate shear strength of end-web panels. The proposed expression was assessed by comparison to current AISC design rules [10] and ultimate shear strength equations proposed by Lee and Yoo [1].

2 Finite Element Modelling and Verification

Figure 1 illustrates the geometric configuration of a plate girder provided with one-sided intermediate stiffeners and single pair end-bearing stiffeners. The width of end-panel, a, was set equal to web depth, h, of 1500 mm whereas the spacing between intermediate stiffeners was progressively reduced from edges to mid-span to initiate shear failure at the end-panel. The ratio of the flange thickness to web thickness, t_f/t_w, was set equal to 2 whereas the web slenderness ratio, h/t_w, was assumed to be 180. End-bearing and intermediate stiffeners were proportioned to satisfy area and inertia requirements stipulated by the AISC [10]. Material properties were: modulus of elasticity, E = 210 GPa, yield stress, F_y = 240 MPa and Poisson's ratio, μ = 0.30. The plate girder was simply supported at both ends and loaded at mid-span as shown in Figure 1. The top flange was laterally braced at mid-span.

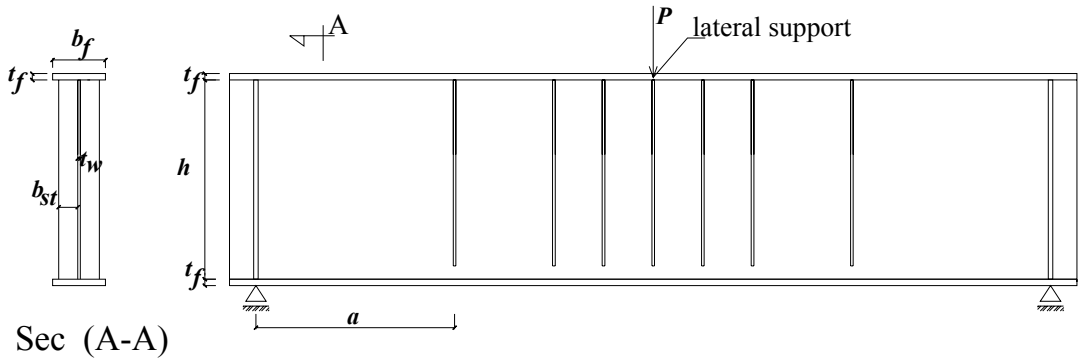

Figure 1: Geometric Configuration of Transversally Stiffened Plate Girder

The finite element model of the plate girder was built using the finite element software ANSYS [16]. All plate elements were modelled with the four noded iso-parametric shell element, Shell 181, in ANSYS element library to account for stress stiffening and large deformations [16]. One half of the plate girder was included in the model due to symmetry. Nodes at the bottom flange at location of support were restrained in vertical direction whereas symmetry boundary conditions were applied at nodes at mid-span. Nodes at the top flange at mid-span were restrained in the out-

of-plane to mimic lateral bracing of the plate girder. Loading was applied as vertical nodal forces along the web depth at mid-span to exclude failure due to local web yielding.

The elastic buckling load, V_{cr}, and ultimate load, V_n, were computed using four mesh configurations (see Figure 2) at which the element size was progressively reduced from 150 mm to 25 mm to select the element size at which the numerical solution was converged. The value of V_{cr} was obtained by solving an Eigen value problem whereas V_n was obtained by conducting inelastic buckling analysis [16]. The inelastic buckling analysis is essentially non-linear static analysis that incorporates geometric and material non-linearities with the assumption of an elastic-perfectly plastic constitutive relation. The Von-Mises yield criterion was adopted to account for material non-linearity [7]. Since out-of-plane deformations can not occur in a flat perfect plate, an initial imperfection having the same shape of the first buckling mode was applied with minute amplitude of $h/12000$ to initiate out-of-plane deformations. Since the AISC allows a maximum deviation from flatness of $h/120$, the plate girder considered herein is counted perfect. Figure 3 shows the convergence of V_{cr} and V_n with the reduction in element size. Results were normalized with the yield load, $V_y = 0.58\ F_y\ h\ t_w$ [7]. The value of V_{cr}/V_y and V_n/V_y was reduced by 0.8% and 2% respectively when the element size was reduced from 50 mm to 25 mm. Therefore, it was concluded that the numerical solution was converged at an element size not more than 50 mm (i.e. Mesh C).

The finite element model was verified by comparison to test results on six plate girders [3]. Dimensions and properties of the six plate girders with F_y of 289.1 MPa were listed in Table 1. Similar to previous results [5, 6], the elastic buckling load, V_{cr}, computed by ANSYS was bound by theoretical buckling load assuming simply supported and fixed boundary conditions at flanges (see Table 2). On the other hand, the value of V_{cr} computed by ANSYS was slightly less than V_{cr} proposed by Lee and Yoo [9] assuming 80% fixation at flanges.

No	Dimensions (mm)						Properties				
	H	a	t_f	t_w	b_s	t_s	h/t_w	a/h	t_f/t_w	I/I_o	b_s/t_s
PG1	600	600	15	3.2	35	3.2	187.5	1	4.69	4.65	10.94
PG2	600	600	15	3.2	40	3.2	187.5	1	4.69	6.94	12.5
PG3	600	600	20	4.0	30	4.0	150	1	5	1.88	7.5
PG4	600	600	20	4.0	45	4.0	150	1	5	6.33	11.25
PG5	600	450	15	3.2	45	3.2	187.5	0.75	4.69	2.70	14.06
PG6	600	450	15	3.2	60	3.2	187.5	0.75	4.69	6.39	18.75

Table 1: Dimensions and section properties of specimens tested by Lee and Yoo [3]

No	V_{cr} (ANSYS)	V_{cr} Theory – Equation (1)		V_{cr} Equation (4)
		Simple- Equation (2)	Fixed - Equation (3)	
PG1	116.7	96.8	130.6	123.8
PG2	118.1	96.8	130.6	123.8
PG3	226.7	189.1	255.1	241.9
PG4	228.2	189.1	255.1	241.9
PG5	150.9	139.9	159.9	155.9
PG6	151.7	139.9	159.9	155.9

Table 2: Assessment of Elastic Buckling Load Results in KN

The ultimate shear strength, V_n, computed by ANSYS compared well with test results such that the difference between test and finite element solution did not exceed 10% as listed in Table 3. Unlike the AISC assumption that tension field action can not develop in end web panels, the numerical solution, however, demonstrated that end web panels possessed significant post-buckling strength. Therefore, V_n stipulated by the AISC rules was indeed conservative as shown in Table 2.

Model	PG1	PG2	PG3	PG4	PG5	PG6
V_n (test) (KN) [3]	204.0	204.5	323.5	333.9	241.6	255.0
V_n (ANSYS) (KN)	206.7	206.8	298.5	299.2	232.2	232.5
V_n (AISC) (KN)	97.1	97.1	189.6	189.6	134.8	134.8
V_{pb} (ANSYS) (KN)	90.1	88.7	71.9	71.0	81.2	80.8

Table 3: Assessment of Inelastic Buckling Analysis Results

Figure 4 illustrates the load versus out-of-plane displacements of PG1; it was shown that displacements were progressively increased when V_{cr} was reached and that the web possessed a significant post-buckling strength of 0.28 V_y (see Tables 3). Figure 5 illustrates the contour plot of middle surface maximum principal stress, S_{max}, in the end panel at ultimate load, the value of S_{max} was peaked at diagonal tension strip and did not reach F_y due to the effect through thickness stresses associated with out-of-plane displacement of the web. Examination of minimum principal stresses, S_{min}, at ultimate load in Figure 6 revealed that compressive stresses were peaked at end-bearing stiffener and reached F_y. On the other hand, the web supported compressive stresses at the vicinity of intermediate stiffener and top flange. Figure 7 illustrates the growth of peak S_{max} and S_{min} in the web, vertical compressive stresses near intermediate stiffeners, S_y, horizontal compressive stresses near top flange, S_x, and vertical stresses in end-bearing stiffener, $S_{y\text{-}stiffener}$, during loading. Unlike most post-buckling theories, the numerical solution revealed that end web panels developed compressive stress field after buckling along stiffeners and top flange to balance with diagonal tension [11-13, 15]. A portion of the diagonal tension was also supported by compressive force in the end-bearing stiffener.

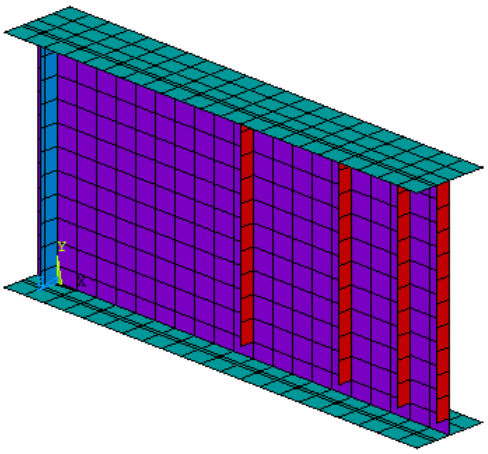

Mesh A (150x150 mm)

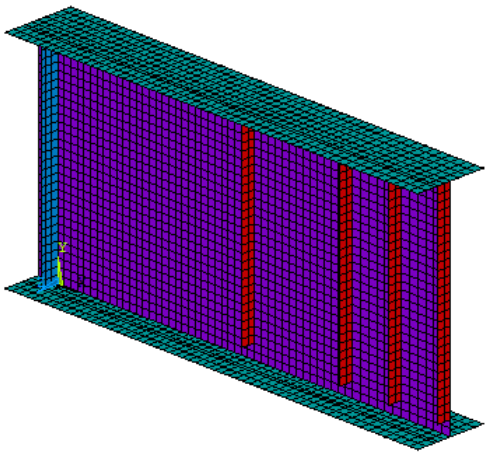

Mesh C (50x50 mm)

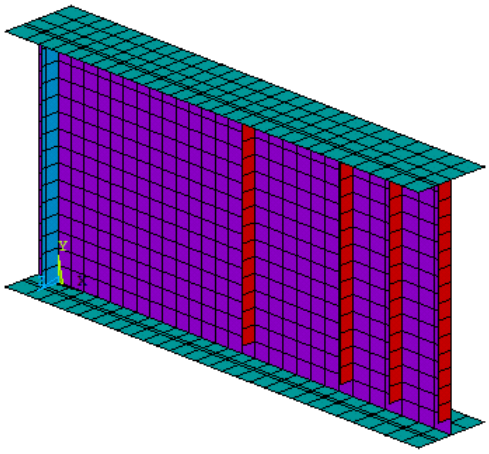

Mesh B (100x100 mm)

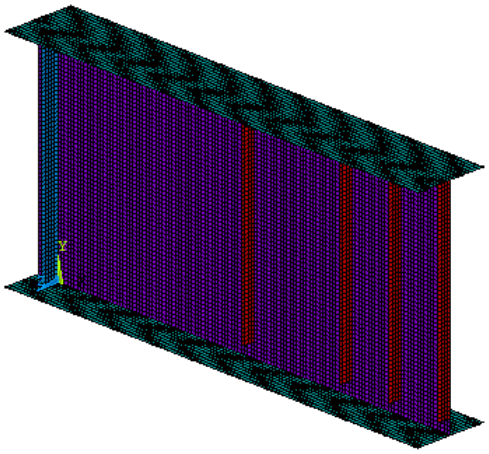

Mesh D (25x25 mm)

Figure 2: Finite Element Models of Plate Girder

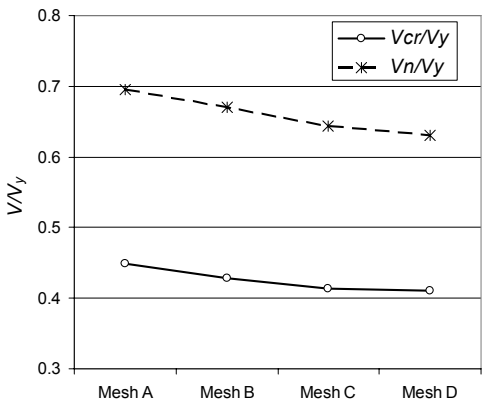

Figure 3: Mesh sensitivity study results

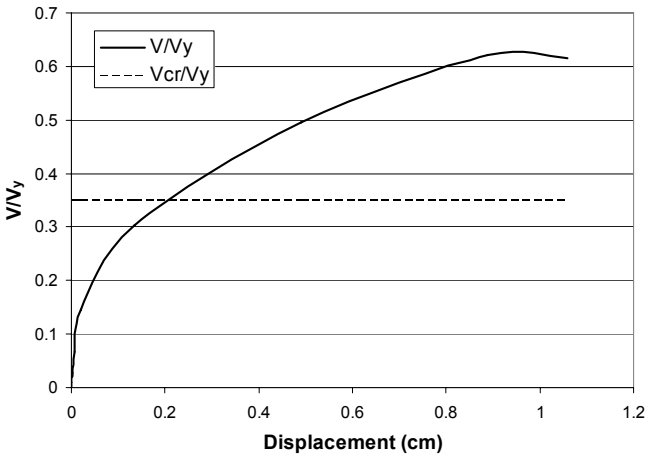

Figure 4: Load deflection curve, PG1

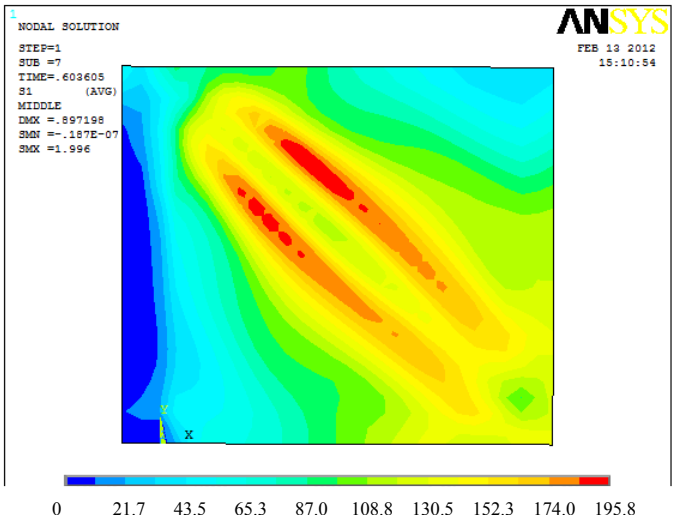

Figure 5: Maximum Principal stresses (MPa) in the web at ultimate load, PG1

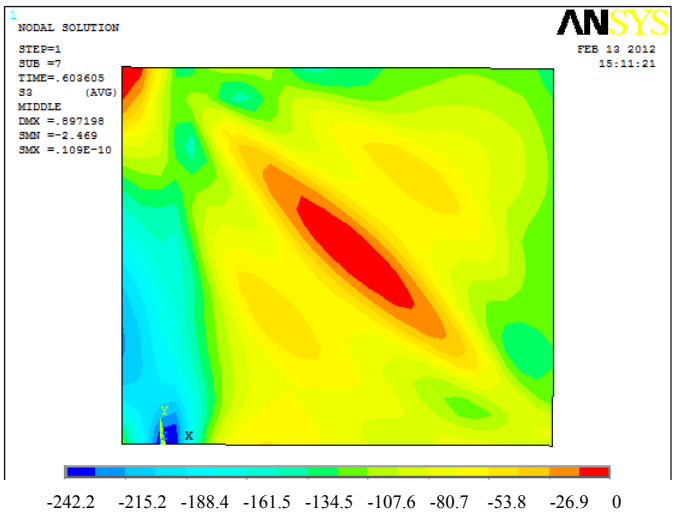

Figure 6: Minimum Principal stresses in the web (MPa) at ultimate load, PG1

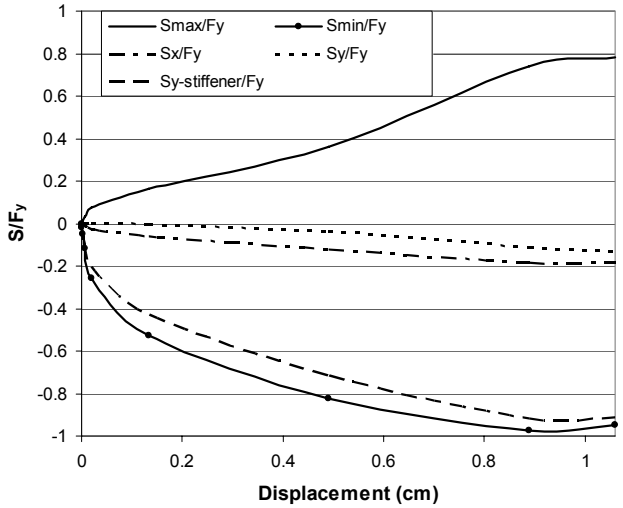

Figure 7: Growth of stresses in end-web panel, PG1

3 Effect of End-Bearing Stiffener Configuration

In this section, the effect of end-bearing stiffener geometric configuration on shear strength of end-web panels was examined considering the plate girder dimensions used in the mesh sensitivity study (Sec. 2). The buckling load, V_{cr} and ultimate shear load, V_n were obtained for four plate girders with no stiffener, one-sided end-bearing stiffener, single pair end-bearing stiffener and doubler end-bearing stiffener as depicted in Figure 8. The post-buckling strength, V_{pb} was also computed as the difference between V_n and V_{cr}. Figure 9 compares V_{cr}, V_{pb} and V_n computed for the four configurations where V_{cr}, V_n and V_{pb} was normalized with V_y. Numerical results indicated that no post-buckling strength can develop when end-bearing stiffener was removed. The value of V_{pb} was almost doubled when single pair end-bearing stiffener was used instead of one-sided end-bearing stiffener. On the other hand, the use of double end-bearing stiffener did not significantly increase V_{pb} and V_n obtained when single pair end-bearing stiffener was utilized. Therefore, it was decided to use single pair end-bearing stiffener in the remainder of this work.

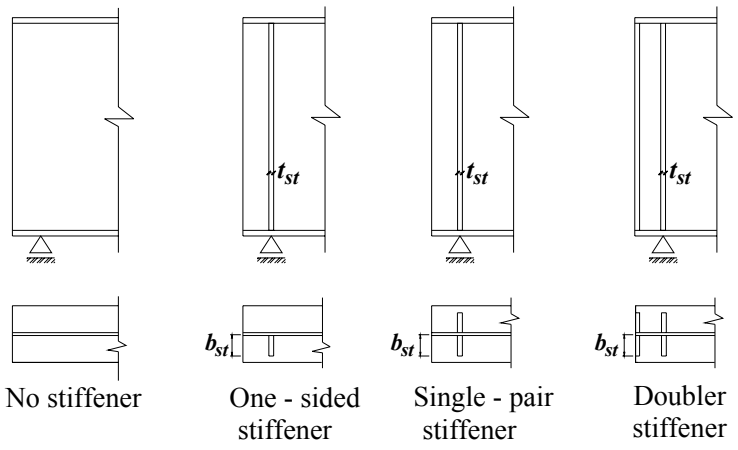

Figure 8: Types of End-Bearing Stiffeners

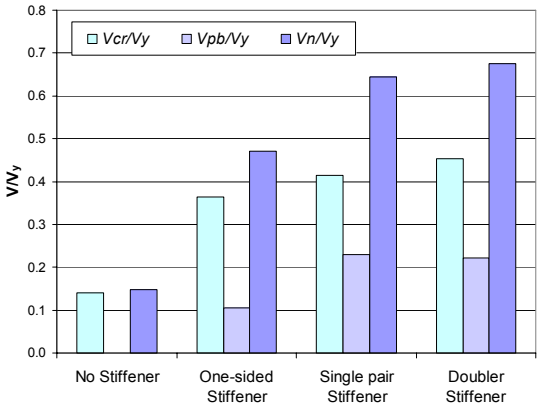

Figure 9: Effect of End-Bearing Stiffener Configuration on Shear Strength

4 Parametric Analysis and Mathematical Formulation

The finite element model established in Sec 2 was used to conduct a parametric analysis to assess the effect of web panel geometric configuration on shear strength of end-web panels. Independent parameters considered herein were: web slenderness ratio, h/t_w, web panel aspect ratio, a/h, ratio of flange to web plate thickness, t_f/t_w, and ratio of intermediate stiffener inertia to required inertia, I/I_o. The dimensions of the end-bearing stiffener was selected to satisfy the area and inertia requirements (Sec. 1) stipulated by the AISC whereas the yield stress, F_y, was set to 240 MPa. The independent parameters considered herein were varied through a wide range of practical values to investigate their effect on V_{cr}, V_{pb} and V_n of end-web panels.

4.1 Elastic buckling strength

Figure 9 shows that the inertia of intermediate stiffeners had minor effect on V_{cr} as long as $I \geq I_o$. for a/h increased from 1 to 5. V_{cr} was reduced significantly at lower web slenderness ratio as depicted in Figure 10. The value of V_{cr} was proportional to t_f/t_w due to increase in rotational restraint provided by flanges when thicker flanges were used [1, 5] (see Figure 11). Therefore, the percentage fixation of the web at flanges measured by the ratio $(K-K_{ss})/(K_{sf}-K_{ss})$ was expressed in terms of t_f/t_w by curve fitting numerical results (see Figure 12). The following expression was obtained:

$$K = K_{ss} + (0.09\ t_f/t_w + 0.3)\ (K_{sf}-K_{ss}) \quad \leq K_{sf} \qquad (13)$$

The proposed K coefficient of Equation (13) , K-Proposed, was compared to the buckling coefficient obtained from numerical solution, K-ANSYS, buckling coefficient stipulated by AISC (Equation (5)), K-AISC, and the buckling coefficient assuming 80% fixation (Equation (4)), K-Lee, in Figures 13 and 14 for t_f/t_w = 2 and 6 respectively and h/t_w = 180. Both K-Lee and K-proposed provided good estimate of numerical results, however, K-proposed provided better correlation with numerical results at t_f/t_w= 2. On the other hand, the AISC underestimated numerical results by 30% on average. [10].

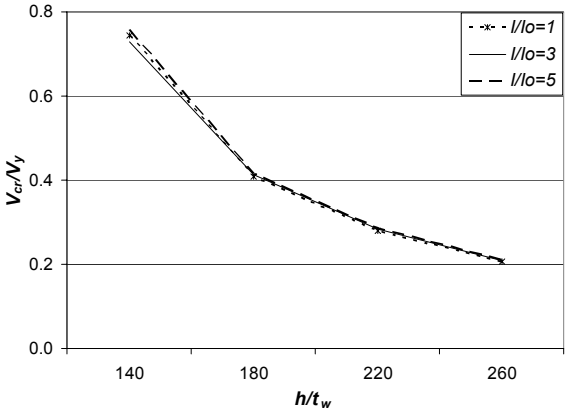

Figure 9: Effect of I/I_o on V_{cr}/V_y (a/h=1)

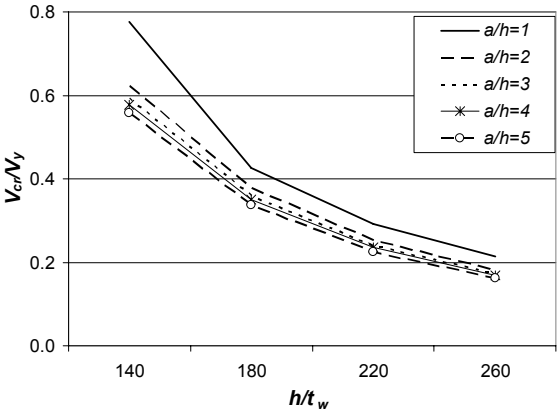

Figure 10: Effect of a/h on V_{cr}/V_y (t_f/t_w =4)

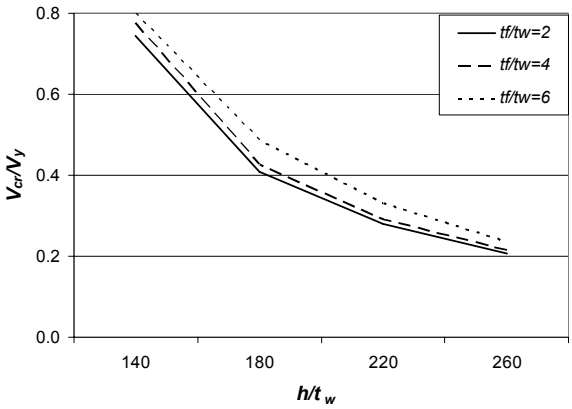

Figure 11: Effect of t_f/t_w on V_{cr}/V_y (a/h=1)

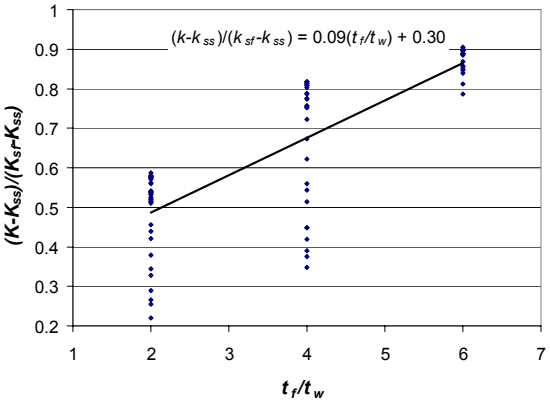

Figure 12: Determination of K coefficient

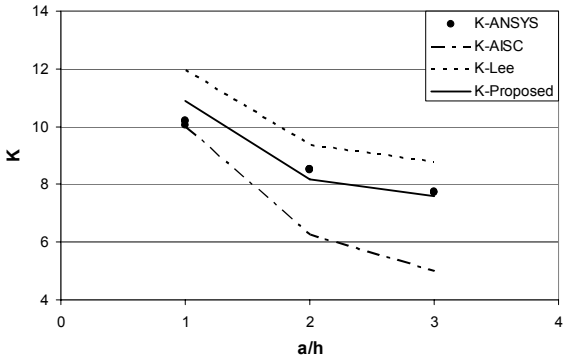

Figure 13: K coefficient for t_f/t_w = 2

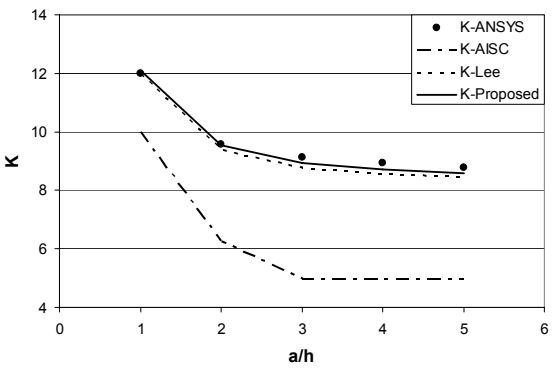

Figure 14: K coefficient for t_f/t_w = 6

4.2 Post-buckling strength

Figure 15 illustrates the variation of $V_{pb}/(V_y\text{-}V_{cr})$ with a/h, I/I_o and non-dimensional web slenderness parameter, $\lambda = \frac{h}{t_w}\sqrt{\frac{F_y}{EK}}$ at t_f/t_w =2. It was shown that V_{pb} was inversely proportional to a/h whereas the inertia of intermediate stiffeners had insignificant effect as long as $I \geq I_o$ and end-bearing stiffeners satisfied area and inertia requirements stipulated by the AISC. The post buckling strength was pronounced when the web slenderness ratio exceeded the elastic buckling limit of 1.39 (see Equations (7) and (9)). Figures 16 to 18 illustrate the variation of V_{pb} with a/h and λ when t_f/t_w was increased from 2 to 6 for I/I_o=1. Unlike the AISC assumption that V_{pb} can not develop in long web panels, numerical results showed that end web panels achieved a post buckling strength in the order of $0.30(V_y\text{-}V_{cr})$ at $3 \leq a/h \leq 5$ and $0.40(V_y\text{-}V_{cr})$ at a/h = 1. Numerical results were used to develop an expression for V_{pb} as follows:

$$\frac{V_{pb}}{(V_y - V_{cr})} = \frac{0.6}{(a/h)+12}\sqrt[6]{\frac{EK}{F_y}\left(\lambda^2 - 1.932\right)} \qquad (14)$$

where K is the buckling coefficient determined from Equation (10). The proposed expression for V_{pb} was compared to numerical results in Figures 16 to 18 for a/h ranging from 1 to 5 and t_f/t_w ranging from 2 to 6. It was shown that Equation (11) estimated the trend of variation of V_{pb} with a/h and λ and was conservative compared to numerical results. Figure 20 shows that the ratio of V_{pb} obtained from Equation (14) to that computed by ANSYS varied from 1.00 to 0.55 with a mean value of 0.72 for all plate girders included in the parametric analysis.

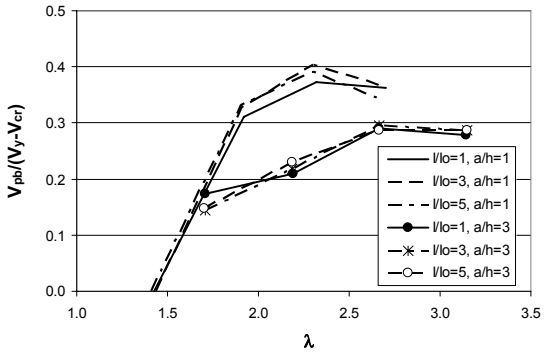

Figure 15: Effect of I/I_o on V_{pb} (t_f/t_w= 2)

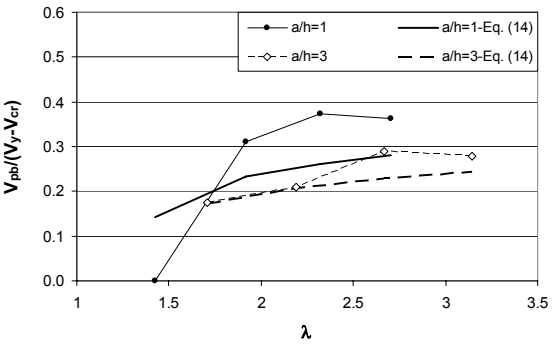

Figure 16: Effect of a/h on V_{pb} (t_f/t_w=2)

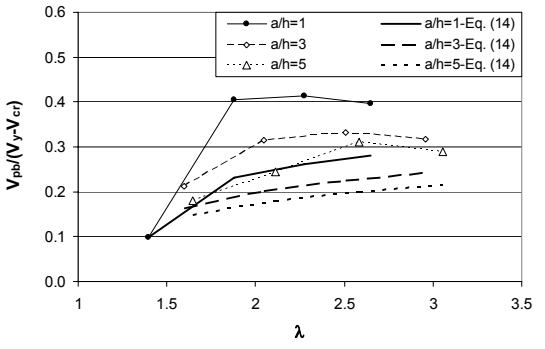

Figure 17: Effect of a/h on V_{pb} (t_f/t_w=4)

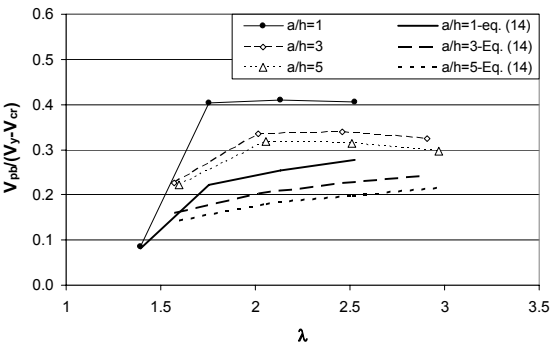

Figure 18: Effect of a/h on V_{pb} (t_f/t_w=6)

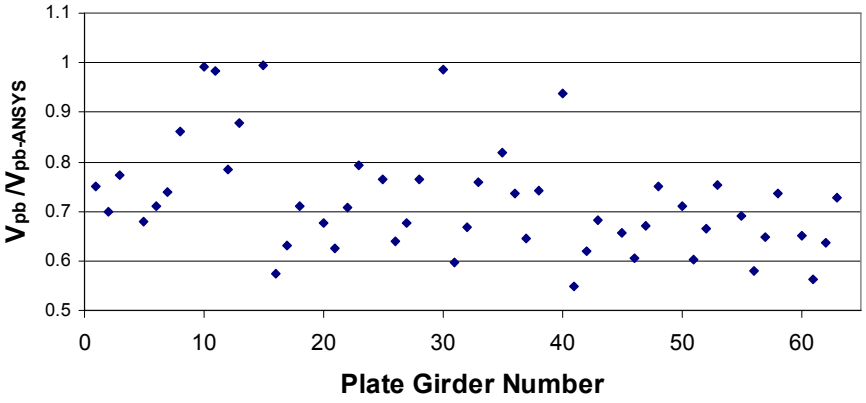

Figure 19: Comparison of V_{pb} computed by Equation (14) to numerical results

4.3 Ultimate Shear Strength

The ultimate shear strength of end web panels obtained from the numerical solution was compared to the AISC design rules in Figures 20 to 22 for I/I_o =1 and t_f/t_w= 2 to 6. Although the AISC conservatively assumed the web to be simply supported at flanges, it was shown that the AISC design rules underestimated V_n of end web panels by 40% on average by neglecting its post-buckling strength.

Since the ultimate shear strength is the sum of elastic buckling strength and post-buckling strength, an expression for the ultimate shear strength of end web panels was established using Equations 13 and 14 as follows:

For $\lambda \le 1.112$ $V_n = V_y$ (15a)

For $1.112 \le \lambda \le 1.39$ $V_n = \dfrac{1.112}{\lambda} V_y$ (15b)

For $\lambda \ge 1.39$ $V_n = V_y \left[\dfrac{1.546}{\lambda^2} + \dfrac{0.6}{(a/h)+12} \left(1 - \dfrac{1.546}{\lambda^2}\right) \sqrt[6]{\dfrac{EK}{F_y}\left(\lambda^2 - 1.932\right)} \right]$ (15c)

Figures 23 to 25 compares V_n determined by Equation (15), numerical results and Equation (9) proposed by Lee and Yoo [1]. Evaluation of results indicated that although Equation (9) agreed well with numerical results it overestimated V_n at a/h >1 and/or t_f/t_w =2. On the other hand, Equation (15) agreed well with numerical results for the whole range of geometric configurations studied herein and were biased towards the conservative side. The ratio of V_n of Equation (15) and numerical results varied from 0.83 to 1.09 with a mean value of 0.90 for all plate girders studied herein. Figures 26 to 30 illustrate a comparison between the proposed shear strength equations for V_n and AISC design rules for the whole range of λ for t_f/t_w = 4

and I/I_o = 1. It was shown that Equations (15) provided reasonable estimate of shear strength of end web panels.

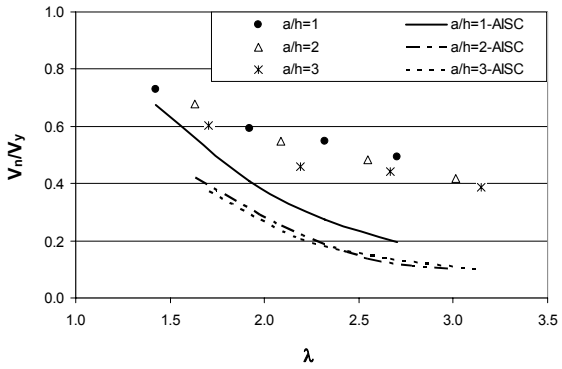

Figure 20: Comparison of AISC to ANSYS results (t_f/t_w =2)

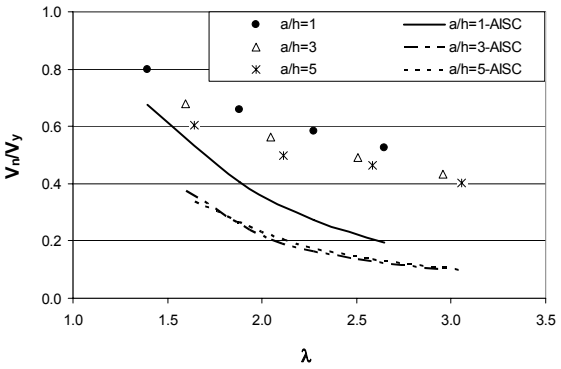

Figure 21: Comparison of AISC to ANSYS results (t_f/t_w =4)

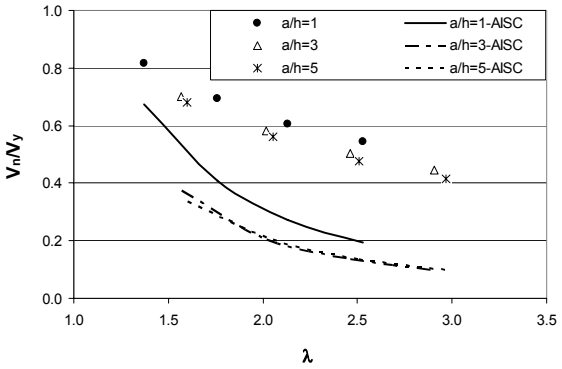

Figure 22: Comparison of AISC to ANSYS results (t_f/t_w =6)

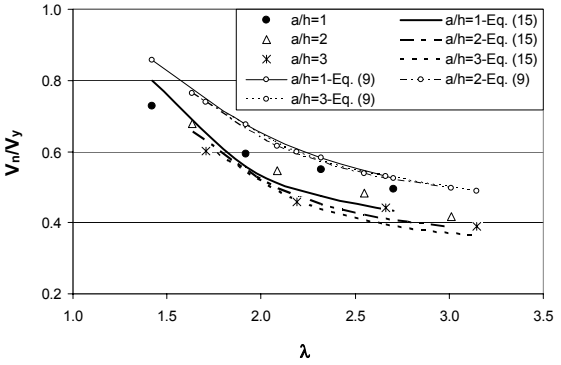

Figure 23: Comparison of Equation (15) to ANSYS and Equation (9) (t_f/t_w=2)

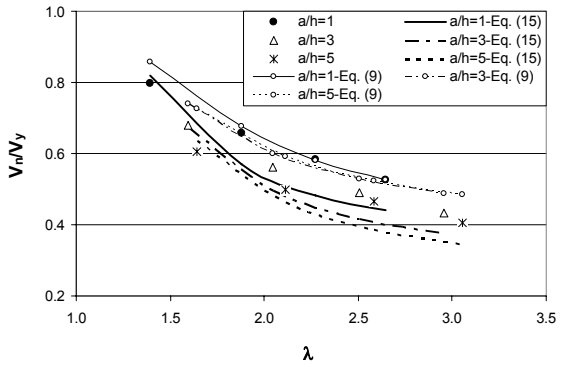

Figure 24: Comparison of Equation (15) to ANSYS and Equation (9) (t_f/t_w =4)

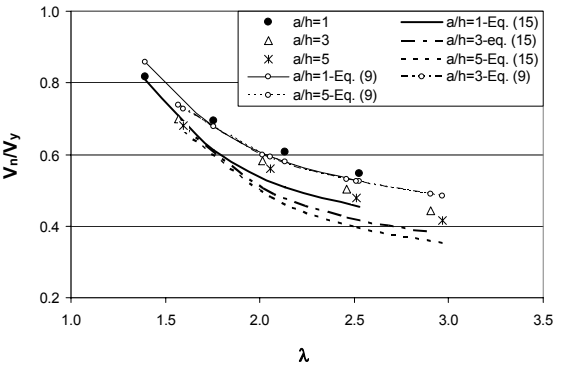

Figure 25: Comparison of Equation (15) to ANSYS and Equation (9) (t_f/t_w=6)

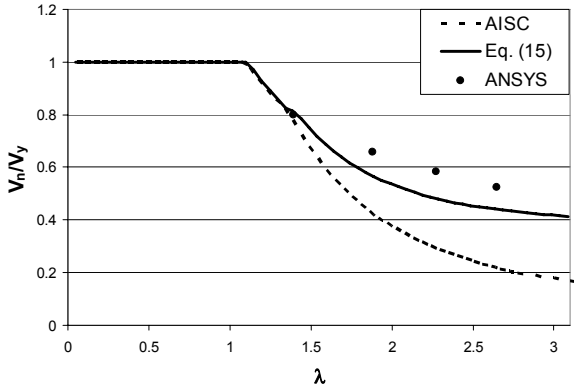

Figure 26: Assessment of Equation (15) for *a/h*=1

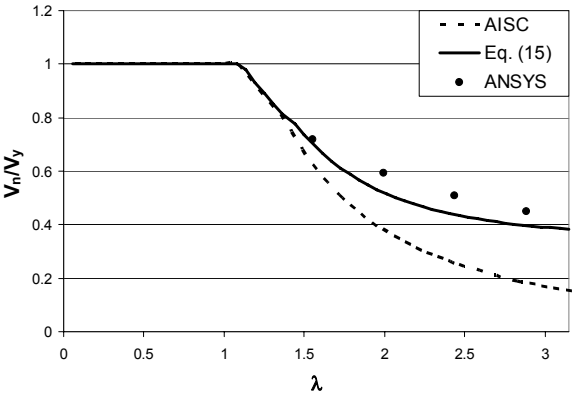

Figure 27: Assessment of Equation (15) for *a/h*=2

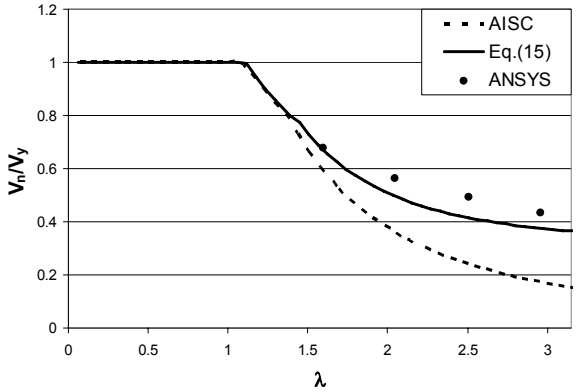

Figure 28: Assessment of Equation (15) for *a/h*=3

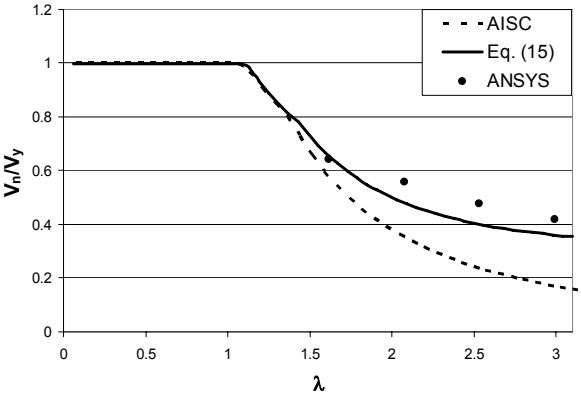

Figure 29: Assessment of Equation (15) for *a/h*=4

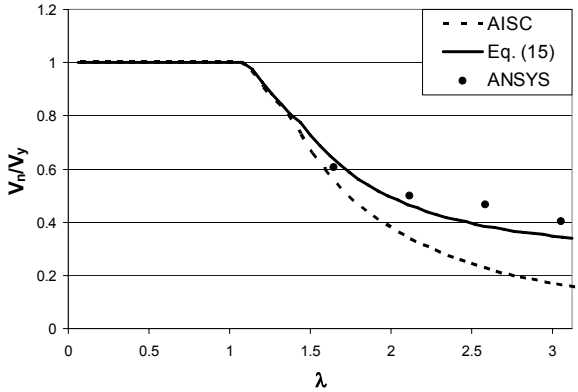

Figure 30: Assessment of Equation (15) for *a/h*=5

5 Summary and Conclusion

In this paper the finite element analysis of end web panels was conducted using the general-purpose finite element software, ANSYS. All plate elements in the exterior panels of a simply supported plate girder were modelled with the iso-parametric finite strain shell element, Shell 181, from the ANSYS element library. End-bearing and intermediate stiffeners were proportioned to satisfy area and inertia requirements stipulated by the AISC specifications. The suitable element size that provided converged elastic buckling load and ultimate load was determined by a mesh sensitivity study at which the size of elements was progressively reduced. The finite element model established herein was verified by comparing elastic buckling load to classical theory whereas ultimate load was compared to test results on six plate girders published in literature [3]. The effect of end-bearing stiffeners on shear strength of end web panels was investigated by studying four plate girders cases with no end-bearing stiffener, one-sided end bearing stiffener, single pair end-bearing stiffener and doubler end-bearing stiffener. It was shown that single pair end-bearing stiffener increased significantly the shear strength of end-web panels compared to one-sided end-bearing stiffener. On the other hand, no significant increase in ultimate shear strength was noticed when doubler end-bearing stiffener was used compared to single pair end bearing stiffener. An extensive parametric analysis was conducted to investigate the effect of: web slenderness ratio, panel aspect ratio, inertia of intermediate stiffeners and ratio of flange to web thickness on shear strength of end web panels stiffened with single pair end-bearing stiffener and one sided intermediate stiffeners. Numerical results of more than sixty plate girders were used to establish an expression elastic buckling coefficient, post-buckling strength and ultimate strength of transversally stiffened end web panels. The proposed expressions were compared to AISC, numerical results and mathematical models proposed by Lee and Yoo [1]. The proposed expressions provided good estimate of numerical results compared to AISC design rules. Based on this work, the following can be concluded for the range of parameters considered herein:

- Unlike Basler's theory and AISC design assumptions, end web panels stiffened with adequately designed end-bearing and intermediate stiffeners can support shear loads after web buckling at which diagonal tension forces are balanced by compressive forces supported by end-bearing stiffener and portions of the web stiffened by upper flange and stiffeners.
- Unlike the arbitrary assumption that web panels with aspect ratio, a/h, greater than 3 can not possess post-buckling strength, it was shown that stiffened end web panels with $3 \leq a/h \leq 5$ possessed significant post-buckling strength that ranged from 0.15 to 0.30 ($V_y - V_{cr}$).
- The inertia and area requirements of end-bearing stiffeners stipulated by AISC design rules were sufficient to produce post-buckling strength in end web panels.
- Elastic buckling analysis on sixty four plate girders showed that the boundary condition of the web at flanges were closer to fixation compared to simple supports. Flanges with t_f/t_w ranging from 2 to 6 provided 22% to 90% fixation to

web. A mathematical expression for web buckling coefficient was established to account for the effect of t_f/t_w and a/h on elastic buckling strength of end web panels.

- Inelastic buckling analysis on sixty four plate girders showed that the post-buckling strength of end web panels was inversely proportional to a/h and was pronounced, however, at higher web slenderness ratios (i.e. $\lambda > 1.39$) and/or greater t_f/t_w ratios. An expression for post-buckling strength was established incorporating the effect of: a/h, λ and t_f/t_w.
- An expression for ultimate shear strength for end web panels was established based on mathematical models of K and V_{pb}. The proposed expression of V_n provided a good estimate of numerical results compared to design rules adopted by AISC specifications [10] and design rules proposed by Lee and Yoo [1].

References

[1] Lee, S. C., and Yoo, C. H., "Strength of Plate Girder Web Panels Under Pure Shear", Journal of Structural Engineering, ASCE, 124, 184-194, 1998.

[2] Lee, S.C. and Yoo, C.H., "Experimental Study on Ultimate Shear Strength of Web Panels", Journal of Structural Engineering, ASCE, 125, 838-46, 1999.

[3] Lee, S.C., Yoo, C.H. and Yoon, D.H. "New Design Rule for Intermediate Transverse Stiffeners Attached to Web Panels", Journal of Structural Engineering, ASCE, 129, 1607- 1614, 2003.

[4] Shanmugan, N.E. and Baskar, K. "Steel-Concrete Composite Plate Girders Subjected to Shear Loading", Journal of Structural Engineering, ASCE, 129, 1230-41, 2003.

[5] Machaly, E.B., Safar, S.S. and Abdel Nabi, A.E., "Parametric Analysis of Plate Girder Web Plates Subjected to Pure Shear", Journal of Engineering and Applied Sciences, Cairo University, 54, 617-634, 2007.

[6] Machaly, E.B., Safar, S.S. and Abdel Nabi, A.E., " New Design Rules for Plate Girder Web Panels Subjected to Pure Shear", Journal of Engineering and Applied Sciences, Cairo University, Vol. 55, 21-40, 2008.

[7] Salmon, C.G. and Johnson, J.E.," Steel Structures: Behaviour and Design", Harper and Row Publishers, 4th Edition, 1996.

[8] Timoshenko, S. P., and Gere, J. M., "Theory of elastic stability", 2nd Ed., McGraw-Hill Book Co., Inc., New York, N. Y., 1961.

[9] Lee, S. C., Davidson, J. S., and Yoo, C. H. "Shear buckling coefficient of plate girder web panels", Computers and Structures, 59, 789-795, 1996.

[10] American Institute of Steel Construction specification for structural steel buildings, Load and Resistance Factor Design. AISC, Chicago, III, 2005.

[11] Lee, S.C. and Yoo. C.H.," Mechanics of Web Panel Post-Buckling in Shear", Journal of Structural Engineering, ASCE, 132, 1580-89, 2006.

[12] Lee, S.C., Lee, D.S. and Yoo, C.H., "Further insights into Post-buckling of Web Panels: I. Review of Flange Anchoring Mechanism", Journal of Structural Engineering, ASCE, 135, 3-10, 2009.

[13] Lee, S.C., Lee, D.S., Park, C.S. and Yoo, C.H., "Further insights into Post-buckling of Web Panels: II Experiments and Verification of New Theory", Journal of Structural Engineering, ASCE, 135, 11-18, 2009.
[14] Alinia, M.M., Shakiba, M., and Habashi, H.R., "Shear Failure Characteristic of Steel Plate Girders", Thin Walled Structures, 47, 1498-1506, 2009.
[15] Safar, S.S., "Effect of Transverse Stiffeners on Shear Strength of Web Panels", International Bridge Conference, Pittsburgh, Pennsylvania, USA, IBC 11-32, 2011.
[16] Desalvo, G.J., and Gorman, R.W., "ANSYS User's Manual", Swanson Analysis Systems, Houston, PA, 1989.